Letter

Trapping and acceleration of spin-polarized positrons from γ photon splitting in wakefields

Wei-Yuan Liu [1,2,*] Kun Xue [3,*] Feng Wan [3] Min Chen [1,2,†] Jian-Xing Li [3,‡] Feng Liu [1,2]
Su-Ming Weng [1,2] Zheng-Ming Sheng [1,2,4] and Jie Zhang [1,2,4]

[1]*Key Laboratory for Laser Plasmas (MOE), School of Physics and Astronomy, Shanghai Jiao Tong University, Shanghai 200240, China*
[2]*Collaborative Innovation Center of IFSA (CICIFSA), Shanghai Jiao Tong University, Shanghai 200240, China*
[3]*Ministry of Education Key Laboratory for Nonequilibrium Synthesis and Modulation of Condensed Matter, Shaanxi Province Key Laboratory of Quantum Information and Quantum Optoelectronic Devices, School of Physics, Xi'an Jiaotong University, Xi'an 710049, China*
[4]*Tsung-Dao Lee Institute, Shanghai Jiao Tong University, Shanghai 200240, China*

(Received 28 October 2020; revised 29 December 2021; accepted 10 April 2022; published 3 May 2022)

Energetic spin-polarized positrons are very useful for forefront research such as e^-e^+ collider physics, but it is still quite challenging to generate such sources. Here, we propose an efficient scheme of trapping and accelerating polarized positrons in plasma wakefields. By developing a fully spin-resolved Monte Carlo method, we find that in the nonlinear Breit-Wheeler pair production the polarization of intermediate γ photons significantly affects the pair spin polarization, and ignoring this effect would result in an overestimation of the pair yield and polarization degree. In particular, seed electrons colliding with a bichromatic laser create polarized γ photons which split into e^-e^+ pairs via the nonlinear Breit-Wheeler process with an average (partial) positron polarization above 30% (70%). Over 70% of positrons are then trapped and accelerated in the recovered wakefields driven by a hollow electron beam, obtaining an energy gain of 3.5 GeV/cm with slight depolarization. Our method provides the potential for constructing compact polarized positron sources for future applications and may also attract broad interest in strong-field physics, high-energy physics, and particle physics.

DOI: 10.1103/PhysRevResearch.4.L022028

Plasma-based wakefield accelerators have attracted worldwide attention in recent years due to their capability of providing acceleration gradients three orders of magnitude higher than conventional radio-frequency accelerators [1–3]. This promises a new possibility for future electron-positron (e^-e^+) colliders with a relatively compact size and low cost [4–6], in which polarized particles are preferred because they are favorable for observing special chiral couplings and suppressing unwanted reaction channels [7]. Polarized electron sources are mostly based on the photodissociation of hydrogen halides [8] and many proposals for producing polarized electrons from wakefields have been explored [9–11]. Polarized positron sources are commonly generated either via a radiative process (Sokolov-Ternov effect) in a storage ring [12–14] or high-energy polarized γ photons interacting with a high-Z target (Bethe-Heitler pair production) [15]. For the former, the polarization time is rather long since the magnetic fields of a synchrotron are quite weak; for the latter, the positron density is limited by low photon luminosity [16–18]. Recently, state-of-the-art laser pulses with peak intensities up to 10^{22} W/cm^2 [19–22] have enabled the excitation of nonlinear quantum electrodynamics (QED) processes [23,24] in laser-matter interactions [25–28]. Accordingly, GeV-level polarized positron beams can be generated directly from intense laser pulses. It is mainly through the radiative polarization effect in, e.g., a bichromatic laser pulse [29] and an elliptically polarized laser pulse [30] (transverse polarization), or via the helicity transfer from polarized γ photons [31] (longitudinal polarization). Unfortunately, none of the above methods can generate ultrahigh-energy (hundreds of GeV) polarized positron beams for applications in high-energy and particle physics (e.g., a polarized e^-e^+ collider [32]). Therefore, it is important to explore viable schemes to synchronize polarized positrons for acceleration in plasma wakefields. Moreover, the significant impact of the polarization of intermediate γ photons on the pair spin polarization in the nonlinear Breit-Wheeler (BW) process was not considered in Refs. [29,30], and only a particular case for circularly polarized γ photons was taken into account in Ref. [31]. We will discuss generally the effect of γ photon polarization on pair spin polarization in this Letter.

We also underline that the trapping and acceleration of polarized positron beams in plasma wakefields are still quite challenging and rarely studied. Previous schemes [33] for the effective trapping and acceleration of electrons in plasma wakefields [34,35] are not applicable for positrons since the transverse fields in nonlinear wakes usually defocus the positrons. To solve this problem, long positron beams are used to provide head-to-tail energy transfer in self-loaded plasma

*These authors contributed equally to this work.
†minchen@sjtu.edu.cn
‡jianxing@xjtu.edu.cn

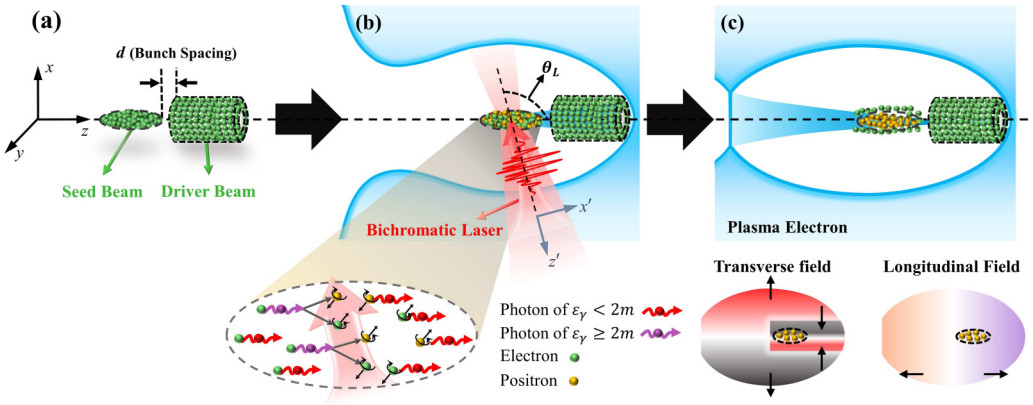

FIG. 1. Interaction scenario of polarization, trapping, and acceleration of positrons. (a) A hollow electron beam copropagates with a seed electron beam along the $+z$ direction with a separation distance d. (b) A LP bichromatic laser pulse, polarizing in the x'-z' plane, collides with the seed beam with a collision angle θ_L and disrupts the bubble. (c) When the laser leaves, the bubble gradually recovers and traps the positrons. During the bubble closing, the transverse fields (red-black gradients) near the bubble axis can focus the positrons and repel the electrons; the front parts of the longitudinal fields (purple-orange gradients) accelerate the positrons and decelerate the electrons. The black arrows indicate the force felt by the positrons due to the wakefields.

wakefields [36]. Shaped drivers [37,38] or plasmas [39–42] enable a region where positrons can be accelerated and simultaneously focused. In these schemes, however, positron beams are assumed to be preloaded and the beam polarization property is neglected.

In this Letter, we propose a compact scheme to generate polarized positrons and inject them into plasma wakefields with further acceleration to high energies (i.e., solving the key difficulties of positron polarization and injection in plasma acceleration). The positron generation and polarization are studied quantum mechanically, while the bubble-recovery-based positron trapping and subsequent acceleration and depolarization in wakefields are studied semiclassically via our developed fully spin-resolved Monte Carlo method. The interaction schematic is shown in Fig. 1. A hollow electron beam working as a wake driver propagates into a low-density plasma and excites nonlinear wakefields (bubbles). Behind it, another copropagating seed electron beam collides with an ultraintense linearly polarized (LP) bichromatic laser pulse to emit abundant LP γ photons via nonlinear Compton scattering, which could further decay into transversely polarized pairs through the nonlinear BW process [see Fig. 1(b)] due to asymmetric pair production and polarization probabilities in the laser positive and negative half cycles. We underline that it is necessary to take the polarization of intermediate γ photons into account. Otherwise, the yield and polarization of positrons will be remarkably overestimated (see Fig. 2). During the collision of the laser and seed beam, the wake structure driven by the driver beam is first destroyed [see Fig. 1(b)] and then gradually self-recovers downstream of the laser-seed beam collision point [see Fig. 1(c)]. Some of the created high-energy polarized positrons can be trapped in the recovered wakefields and then accelerated by the wakefields [see Fig. 1(c)]. In our simulations over 70% positrons are finally injected into the wake and get further accelerated to an average energy beyond 1.2 GeV in 1 mm, with an average polarization exceeding 30%. The partial polarization of the positrons within the full width at half maximum (FWHM)

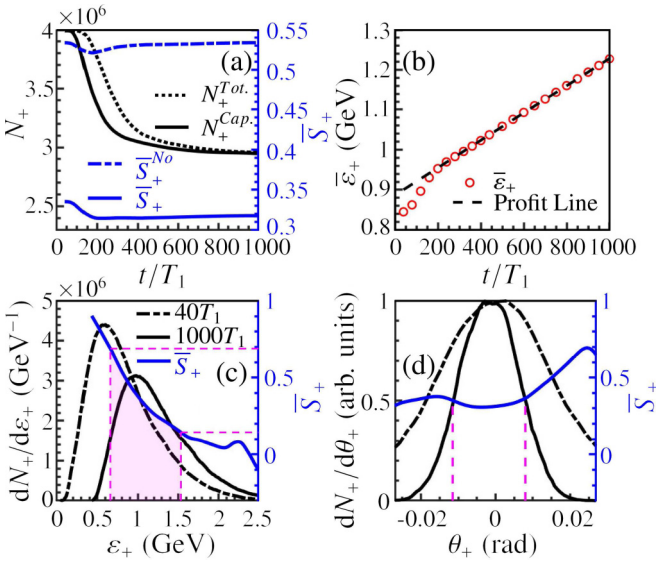

FIG. 2. Evolutions of the total positron number $N_+^{\mathrm{Tot.}}$ inside the first bubble (black dotted), captured positron number inside the focusing region $N_+^{\mathrm{Cap.}}$ (black solid), and average polarization of captured positrons $\overline{S}_+$ (blue solid) by considering the polarization of intermediate γ photons, respectively. The blue dashed-dotted curve ($\overline{S}_+^{\mathrm{No}}$) indicates the average polarization of captured positrons for the case of artificially neglecting the polarization of intermediate γ photons. (b) Average energy of captured positrons $\bar{\varepsilon}_+$ (red circles) and its linear profit (black dashed) vs the interaction time t, respectively, with an acceleration gradient $G \approx 3.58$ GV/cm. (c) Energy spectra of captured positrons $dN_+/d\varepsilon_+$ [at the instant of completing the pair creation $t_i = 40T_1$ (black dashed-dotted) and at the end of the simulation $t_f = 1000T_1$ (black solid)] and $\overline{S}_+$ at t_f (blue solid) vs the positron energy ε_+, respectively. (d) Normalized angular distributions of positrons at t_i (black dashed-dotted) and t_f (black solid), and $\overline{S}_+$ at t_f (blue solid) vs the transverse angular divergence of the positrons $\theta_+ = \arctan(p_{+,x}/p_{+,z})$, respectively. The initial parameters of the laser pulse, electron beams, and plasma are given in the text.

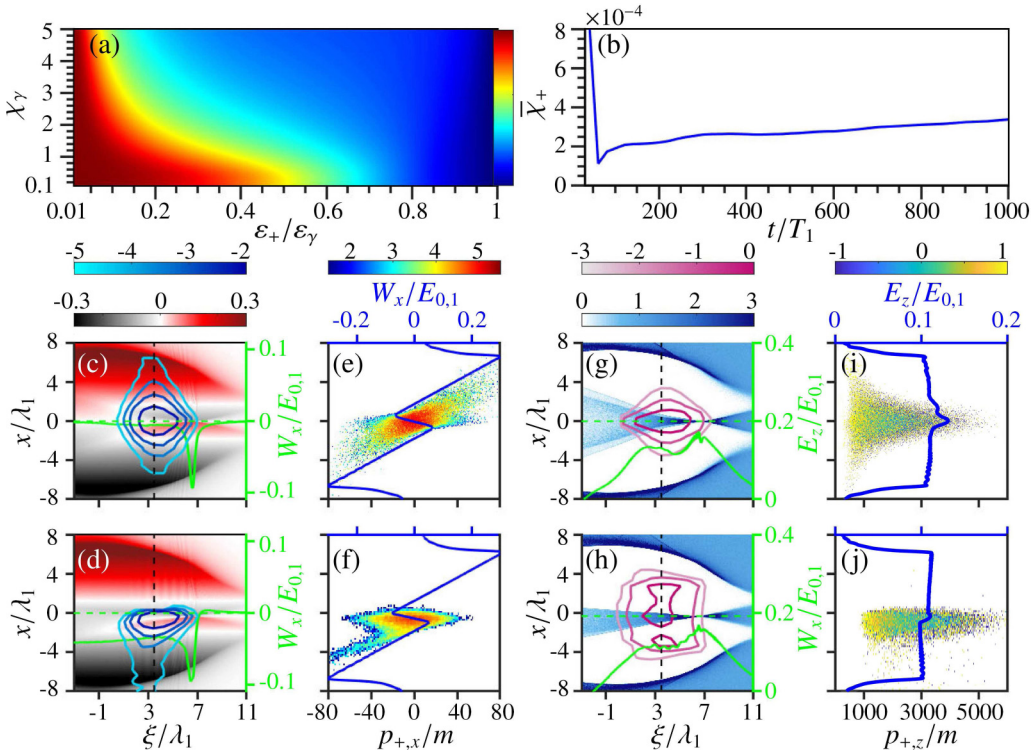

FIG. 3. (a) Analytical value of $\overline{S}_+$ with respect to χ_γ and $\varepsilon_+/\varepsilon_\gamma$; see the analytical expression in the SM [43]. (b) $\overline{\chi}_+$ vs t. (c) [(d)] Focusing fields $W_x = E_x - B_y$ felt by positrons normalized by $E_{0,1} = 2\pi m/\lambda_1 e$ (red-black gradients) and positron density contours $\log_{10}(n_+/n_{p,0})$ (cyan-blue gradients) with respect to the comoving frame variable $\xi = z - t$ and x. The green curve represents the longitudinal distribution of W_x [with $x = x_{\rm wake} + dx$ and $t = 100T_1$ ($t = 1000T_1$), where the bubble axis is at $x_{\rm wake} \approx -0.03\lambda_1$ ($x_{\rm wake} \approx -0.34\lambda_1$)]. E_x and B_y are transverse components of the wakefields, respectively. (e) [(f)] Distribution of the positron number ($\log_{10} N_+$) with respect to $p_{+,x}$ and x. The blue line represents W_x at $\xi = 3.5\lambda_1$ vs x at $t = 100T_1$ ($t = 1000T_1$). (g) [(h)] Distributions of background electron density $n_p/n_{p,0}$ (white-blue gradients) and contours of seed electron density $\log_{10}(n_s/n_{p,0})$ (white-magnet gradients) with respect to ξ and x. The green curve represents the longitudinal electric field E_z at $x = x_{\rm wake} + dx$ vs ξ at $t = 100T_1$ ($t = 1000T_1$). (i) [(j)] Distributions of $\overline{S}_+$ with respect to $p_{+,z}$ and x. The blue curve represents E_z at $\xi = 3.5\lambda_1$ vs x, at $t = 100T_1$ ($t = 1000T_1$). Other parameters are the same with those in Fig. 2.

of the energy spectrum can exceed 70% [see Fig. 2(c)]. The effectiveness of our proposed scheme has been proved for a large range of electron and plasma parameters by three-dimensional (3D) particle-in-cell (PIC) simulations [see more details in the Supplemental Material (SM) [43]]. The detailed injection and acceleration processes are discussed in the following.

We develop a Monte Carlo algorithm and implement it in the two-dimensional (2D) and 3D QED PIC code (benchmarked by the EPOCH code [44]) to describe the creation and polarization of the pairs quantum mechanically by using spin-resolved probabilities of nonlinear BW pair production [43], which are derived from the QED operator method [45] in the local constant field approximation (valid at the invariant laser field parameter $a_0 = |e|E_0/m\omega \gg 1$) [23,46–48]. To efficiently generate γ photons and pairs requires the nonlinear QED parameters $\chi_e \equiv |e|\sqrt{-(F_{\mu\nu}p_e^\nu)^2}/m^3 \gtrsim 1$ (for electrons) and $\chi_\gamma \equiv |e|\sqrt{-(F_{\mu\nu}k_\gamma^\nu)^2}/m^3 \gtrsim 1$ (for γ photons) [23,46]. Here, $F_{\mu\nu}$ is the field tensor, p_e^ν and k_γ^ν the 4-momenta of the electron and γ photon, respectively, e and m the electron charge and mass, respectively, and E_0 and ω the laser amplitude and frequency, respectively. Relativistic units with $c = \hbar = 1$ are used throughout. The simulations of spin-resolved electron (positron) dynamics and photon emission and polarization follow the semiclassical algorithms in Refs. [30,49,50]. See more details of our simulation method in the SM [43].

We carry out 2D simulations to illustrate our scheme, and 3D simulations are only employed to test high-dimensional effects due to computational limitations. The simulation parameters of the laser pulse, electron beams, and plasma are summarized as follows. A tightly focused LP Gaussian bichromatic laser pulse propagates along the $-z'$ direction with $\theta_L = 105^\circ$ and polarizes in the x'-z' plane, with wavelengths $\lambda_1 = 1$ μm (period T_1) and $\lambda_2 = 0.5$ μm, pulse durations $\tau_1 = \tau_2 = 6T_1$, focal radii $w_1 = w_2 = 2$ μm, and peak amplitudes $a_1 = 4a_2 \approx 67$ (corresponding to peak intensities $I_1 = 4I_2 \approx 6.15 \times 10^{21}$ W/cm^2). An unpolarized elliptical seed beam propagates along the $+z$ direction, with an average energy $\varepsilon_{s,0} = 4$ GeV, major axis $L_{\rm maj} = 7$ μm, and minor axis $L_{\rm min} = 2$ μm. A hollow driver beam is initially placed at the entrance of the plasma, with an average energy $\varepsilon_{d,0} = 1$ GeV, outer radius $w_{\rm out} = 3$ μm, inner radius $w_{\rm in} = 1.5$ μm, and length $L_h = 9$ μm. The density, energy spread, and angular divergence of the two electron beams are $n_{s,0} = n_{d,0} = 0.1n_c$ with a Gaussian distribution (the critical density $n_c = 1.1 \times 10^{21}$ cm^{-3} with respect to the laser pulse with a wavelength of λ_1), $\Delta\varepsilon_{s,0}/\varepsilon_{s,0} = \Delta\varepsilon_{d,0}/\varepsilon_{d,0} = 0.1$, and $\Delta\theta_s =$

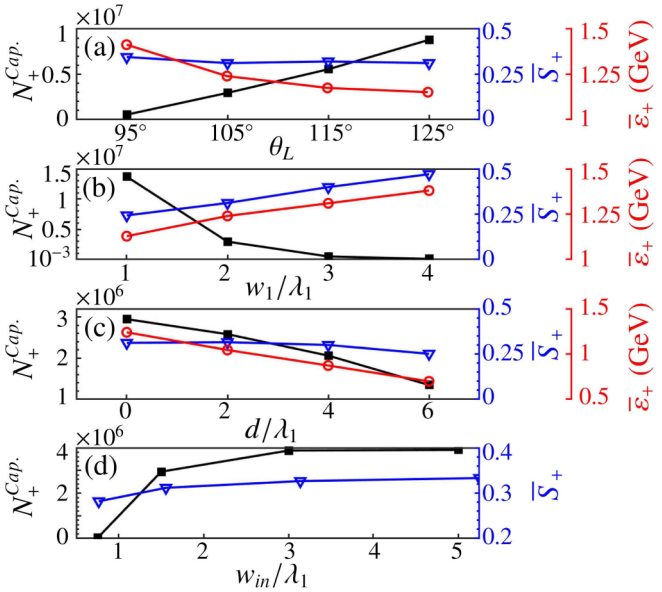

FIG. 4. (a)–(d) Variations of $N_+^{\mathrm{Cap.}}$ (black square), $\overline{S}_+$ (blue triangle), and $\overline{\varepsilon}_+$ (red circle) of captured positrons at t_f with respect to θ_L, w_1 ($w_1 = w_2$ with a fixed laser energy), d, and w_{in}, respectively. Other parameters are the same with those in Fig. 2.

$\Delta\theta_d = 0.1$ mrad, respectively. Here, the delay distance of the two electron beams is $d = 0$ μm [other cases with different d are given in Fig. 4(c)]. More parameter scans for the driver beam size and other effects are shown in Fig. 4. The density of the background plasma (composed of H^+ and electrons) is $n_{p,0} = 0.01n_c$. Note that the efficient excitation of a wakefield with central focusing fields for the positrons requires the driver beam to satisfy $w_{\mathrm{in}}/\sigma_x \geqslant 3$ and $k_p\sigma_z \leqslant 2$ [38,51], where σ_x and σ_z are the transverse and longitudinal sizes of the driver beam and $k_p = 2\pi/\lambda_p$ with $\lambda_p = \sqrt{\pi m/n_{p,0}e^2}$. Here, we use $w_{\mathrm{in}}/\sigma_x = 3$ and $k_p\sigma_z \approx 1.8$, and the simulation domain is $60\lambda_1(x) \times 80\lambda_1(z)$ with grid resolutions $dx = dz = \lambda_1/50$. The main results of the positron trapping, acceleration, and polarization in 2D simulations are shown in Figs. 2 and 3 (corresponding 3D simulation results are given in the SM [43]). The pair production process is completed at a distance of $t_i \approx 40T_1$, where the bubble has not yet fully recovered, and nearly 4×10^6 positrons are created with a yield ratio $N_+/N_s \approx 0.4\%$ (corresponding to a density of $n_+ \sim 10^{-4}n_c$) and an average polarization (mainly along the magnetic field direction y) $\overline{S}_+ \approx 33.52\%$ [see Fig. 2(a)]. As we mentioned before, if the polarization of intermediate γ photons is artificially neglected as usual, $\overline{S}_+$ will be considerably overestimated by exceeding 68% [see the blue dashed-dotted line in Fig. 2(a), $\overline{S}_+^{\mathrm{No}} \approx 53.5\%$ at t_f]. Therefore we include these effects in our simulations and the analytical calculation of positron polarization is shown in Fig. 3(a). The polarization degree is inversely proportional to the positron energy, which affects the final polarization distribution of the accelerated positrons [see Fig. 2(c)]. Since in our case the QED parameter of the positron $\chi_+ \propto a_{\mathrm{wake}}\gamma_+[1 - \cos(\theta_L)] \ll 1$ [see Fig. 3(b)], the radiative depolarization effect is very weak, where a_{wake} represents the invariant field parameter and γ_+ the Lorentz factor of the positron. The depolarization effect derived from the spin procession in the wakefield, mainly governed by the Thomas-Bargmann-Michel-Telegdi equation [52–54] (the Sokolov-Ternov effect and the Stern-Gerlach force are ignorable [55,56]), is also quite weak [9,57]. Consequently, the final positron polarization distribution mainly depends on the initial pair creation process and the conditions for the positron selection during the trapping and continuous acceleration processes. The last two processes rely on the wakefield structure. The positrons inherit transverse momenta $p_{+,x}$ from the seed electrons via intermediate γ photons. During acceleration, the positrons with large $p_{+,x}$ may escape from the central focusing region and are then expelled out of the bubble by the outer defocusing transverse field. The positrons with low $p_{+,x}$ can be continuously trapped in the acceleration phase [see Figs. 3(c)–3(f)]. Finally at $t_f = 1000T_1$ about 74.12% positrons are accelerated with an average energy increase of about 350 MeV in a distance $\lesssim$1 mm, reaching $\overline{\varepsilon}_+ \approx 1.24$ GeV [see Fig. 2(b)], and the acceleration gradient is $G \approx 3.53$ GV/cm [see Figs. 3(g) and 3(h)]. This gradient is about two orders of magnitude higher than that in Ref. [38], where a plasma with lower density is required for easier injection. Positrons are accelerated with only slight depolarization [see Fig. 2(a)], leading to the final average polarization of $\overline{S}_+ \approx 31.77\%$. In the period of $200T_1 \lesssim t \lesssim 1000T_1$ some high-energy positrons with low polarization gradually escape from the focusing region [see Fig. 3(j)], therefore, the polarization increases a little. At t_f the positron polarization distribution around the peak area of the energy spectrum within the FWHM declines approximately from 70% to 15%. Such a distribution provides a possible way to further increase the polarization by the energy-selection technique [58].

Besides the trapping ratio and polarization degree, the energy spread and divergence are also important factors for future applications. In Fig. 2(c), we find that the relative energy spread of the positrons decreases by about 26% after the wake acceleration compared to the instant of the pair creation t_i, while the absolute energy spread does not increase during the acceleration, because the seed beam not only "provides" the pairs but also flattens the local acceleration field [see Figs. 3(g)–3(j)] assuring uniform acceleration and avoiding energy dispersion. The angular divergence of the positron beam is also improved by the focusing field to $\Delta\theta_+ \approx 20$ mrad, which is about 50% lower than that at t_i [see Fig. 2(d)—the polarization is nearly uniform ($\overline{S}_+ \approx 32.67\%$) within the FWHM labeled by the two dashed purple lines]. One can see that there is an asymmetric angular distribution at t_f in Fig. 2(d). This is induced by the unbalanced plasma perturbations [indicated in Figs. 3(d) and 3(f)], originating from the laser incidence from one side.

Finally, we study the impact of the initial parameters on the trapping, acceleration, and polarization of the positrons in Fig. 4 (see more details in the SM [43] as well). As the collision angle θ_L increases from 95° to 125° (see the interaction scenario in Fig. 1), the probabilities of photon emission and pair production (determined by $\chi_e \propto a_0\gamma_e[1 - \cos(\theta_L)]$ and $\chi_\gamma \propto a_0k_\gamma[1 - \cos(\theta_L)]$, respectively) are both enhanced, thus $N_+^{\mathrm{Cap.}}$ increases. At the same time the average energy decreases due to $\overline{\varepsilon}_+ \propto \sum \varepsilon_\gamma/N_+^{\mathrm{Cap.}} \propto \sum \varepsilon_{s,0}/N_+^{\mathrm{Cap.}}$. $\overline{S}_+$

decreases as well since the asymmetry of the spin-resolved pair production probabilities in the laser positive and negative half cycles is weakened and the radiative depolarization effect is enhanced [see Fig. 4(a)]. As the laser focal radius $w_1(w_2)$ increases with a fixed laser energy J, the laser peak amplitude $a_0 \propto \sqrt{J}/w_1$ and $N_+^{\text{Cap.}} \propto a_0^2 \propto J/w_1^2$ decrease, and accordingly, $\overline{S}_+$ and $\overline{\varepsilon}_+$ are both enhanced [see Fig. 4(b)]. As the distance between the seed and driver beams d rises up, more low-energy positrons with high polarization cannot enter the focusing region to be steadily accelerated (i.e., $N_+^{\text{Cap.}}$ and $\overline{S}_+$ both decrease), and the enhancement of the acceleration field by the seed beam [indicated in Figs. 3(g) and 3(h)] is weakened (i.e., $\overline{\varepsilon}_+$ decreases) [see Fig. 4(c)]. Thus, the condition of $d \lesssim \lambda_p/2$ should be satisfied. As the inner radius of the driver beam w_{in} increases (more feasible in experiments), more plasma electrons converge into the hollow region to create a larger transverse size of the focusing region [38,43], therefore, more positrons can be trapped and the depolarization effect induced by the escape of high-polarization positrons is weakened (i.e., $\overline{S}_+$ increases) [see Fig. 4(d) and more details in the SM [43]]. We underline that in our scheme the positrons are transversely polarized and can be used to investigate specific triple gauge couplings and W-physics, and to test the validity of the standard model and for the discovery of "new physics" [59]. Furthermore, an arbitrary spin orientation can be realized through a proper spin rotator [7].

In conclusion, utilizing both advantages of the laser-driven QED process and plasma wakefield acceleration we have proposed a compact scheme for positron polarization, trapping, and acceleration. Dense GeV positron beams with a spin polarization up to 70% and improved beam quality compared with the scheme of a single laser-electron collision can be achieved, in which the polarization of intermediate γ photons in the nonlinear BW process must be considered. This scheme has the potential for testing QED physics with upcoming 10-PW lasers, where the obtained polarized positron beam can be applied to investigate the structural properties of the material [60] and determine the nucleon structure [61]. By using multistaged wakefield acceleration with currently achievable laser facilities, this scheme also provides a possible way to generate highly polarized positron beams with hundreds of GeV energy for future compact research and application platforms of high-energy and particle physics.

This work was supported by National Natural Science Foundation of China (Grants No. 11991074, No. 11874295, No. 11804269, No. 12022506, and No. 11905169), the National Key R&D Program of China (Grant No. 2018YFA0404801), and the Science Challenge Project of China (Grants No. TZ2016099 and TZ2018005).

[1] T. Tajima and J. M. Dawson, Laser Electron Accelerator, Phys. Rev. Lett. **43**, 267 (1979).

[2] P. Chen, J. M. Dawson, R. W. Huff, and T. Katsouleas, Acceleration of Electrons by the Interaction of a Bunched Electron Beam with a Plasma, Phys. Rev. Lett. **54**, 693 (1985).

[3] K. Nakajima, D. Fisher, T. Kawakubo, H. Nakanishi, A. Ogata, Y. Kato, Y. Kitagawa, R. Kodama, K. Mima, H. Shiraga, K. Suzuki, K. Yamakawa, T. Zhang, Y. Sakawa, T. Shoji, Y. Nishida, N. Yugami, M. Downer, and T. Tajima, Observation of Ultrahigh Gradient Electron Acceleration by a Self-Modulated Intense Short Laser Pulse, Phys. Rev. Lett. **74**, 4428 (1995).

[4] W. Leemans and E. Esarey, Laser-driven plasma-wave electron accelerators, Phys. Today **62** (3), 44 (2009).

[5] C. B. Schroeder, E. Esarey, C. G. R. Geddes, C. Benedetti, and W. P. Leemans, Physics considerations for laser-plasma linear colliders, Phys. Rev. ST Accel. Beams **13**, 101301 (2010).

[6] K. Nakajima, J. Wheeler, G. Mourou, and T. Tajima, Novel laser-plasma TeV electron-positron linear colliders, Int. J. Mod. Phys. A **34**, 1943003 (2019).

[7] G. Moortgat-Pick, T. Abe, G. Alexander, B. Ananthanarayan, A. A. Babich, V. Bharadwaj, D. Barber, A. Bartl, A. Brachmann, S. Chen, J. Clarke, J. E. Clendenin, J. Dainton, K. Desch, M. Diehl, B. Dobos, T. Dorland, H. K. Dreiner, H. Eberl, J. Ellis *et al.*, Polarized positrons and electrons at the linear collider, Phys. Rep. **460**, 131 (2008).

[8] T. P. Rakitzis, P. C. Samartzis, R. L. Toomes, T. N. Kitsopoulos, A. Brown, G. G. Balint-Kurti, O. S. Vasyutinskii, and J. A. Beswick, Spin-polarized hydrogen atoms from molecular photodissociation, Science **300**, 1936 (2003).

[9] M. Wen, M. Tamburini, and C. H. Keitel, Polarized Laser-WakeField-Accelerated Kiloampere Electron Beams, Phys. Rev. Lett. **122**, 214801 (2019).

[10] Y. T. Wu, L. L. Ji, X. S. Geng, Q. Yu, N. W. Wang, B. Feng, Z. Guo, W. Q. Wang, C. Y. Qin, X. Yan, L. G. Zhang, J. Thomas, A. Hützen, A. Pukhov, M. Büscher, B. F. Shen, and R. X. Li, Polarized electron acceleration in beam-driven plasma wakefield based on density down-ramp injection, Phys. Rev. E **100**, 043202 (2019).

[11] Z. Nie, F. Li, F. Morales, S. Patchkovskii, O. Smirnova, W. M. An, N. Nambu, D. Matteo, K. A. Marsh, F. Tsung, W. B. Mori, and C. Joshi, *In Situ* Generation of High-Energy Spin-Polarized Electrons in a Beam-Driven Plasma Wakefield Accelerator, Phys. Rev. Lett. **126**, 054801 (2021).

[12] A. A. Sokolov and I. M. Ternov, On polarization and spin effects in the theory of synchrotron radiation, Sov. Phys. Dokl. **8**, 1203 (1964).

[13] V. N. Baier and V. M. Katkov, Radiational polarization of electrons in inhomogeneous magnetic field, Phys. Lett. A **24**, 327 (1967).

[14] V. N. Baier, Radiative polarization of electrons in storage rings, Sov. Phys. Usp. **14**, 695 (1972).

[15] A. Variola, Advanced positron sources, Nucl. Instrum. Methods Phys. Res. Sect. A **740**, 21 (2014).

[16] T. Omori, M. Fukuda, T. Hirose, Y. Kurihara, R. Kuroda, M. Nomura, A. Ohashi, T. Okugi, K. Sakaue, T. Saito, J. Urakawa, M. Washio, and I. Yamazaki, Efficient Propagation of Polarization from Laser Photons to Positrons through Compton Scattering and Electron-Positron Pair Creation, Phys. Rev. Lett. **96**, 114801 (2006).

[17] D. J. Scott, J. A. Clarke, D. E. Baynham, V. Bayliss, T. Bradshaw, G. Burton, A. Brummitt, S. Carr, A. Lintern, J. Rochford, O. Taylor, and Y. Ivanyushenkov, Demonstration of a High-Field Short-Period Superconducting Helical Undulator Suitable for Future TeV-Scale Linear Collider Positron Sources, Phys. Rev. Lett. **107**, 174803 (2011).

[18] D. Abbott, P. Adderley, A. Adeyemi, P. Aguilera, M. Ali, H. Areti, M. Baylac, J. Benesch, G. Bosson, B. Cade, A. Camsonne, L. S. Cardman, J. Clark, P. Cole, S. Covert, C. Cuevas, O. Dadoun, D. Dale, H. Dong, J. Dumas *et al.* (PEPPo Collaboration), Production of Highly Polarized Positrons Using Polarized Electrons at MeV Energies, Phys. Rev. Lett. **116**, 214801 (2016).

[19] S. Gales, K. A. Tanaka, D. L. Balabanski, F. Negoita, D. Stutman, O. Tesileanu, C. A. Ur, D. Ursescu, I. An-drei, S. Ataman, M. O. Cernaianu, L. DAlessi, I. Dancus, B. Diaconescu, N. Djourelov, D. Filipescu, P. Ghenuche, D. G. Ghita, C. Matei, K. Seto *et al.*, The extreme light infrastructure-nuclear physics (ELI-NP) facility: new horizons in physics with 10 PW ultra-intense lasers and 20 MeV brilliant gamma beams, Rep. Prog. Phys. **81**, 094301 (2018).

[20] B. F. Shen, Z. G. Bu, J. C. Xu, T. J. Xu, L. L. Ji, R. X. Li, and Z. Z. Xu, Exploring vacuum birefringence based on a 100 PW laser and an x-ray free electron laser beam, Plasma Phys. Controlled Fusion **60**, 044002 (2018).

[21] J. W. Yoon, C. H. Jeon, J. H. Shin, S. K. Lee, H. W. Lee, I. W. Choi, H. T. Kim, J. H. Sung, and C. H. Nam, Achieving the laser intensity of 5.5×10^{22} W/cm^2 with a wavefront-corrected multi-PW laser, Opt. Express **27**, 20412 (2019).

[22] C. N. Danson, C. Haefner, J. Bromage, T. Butcher, J.-C. F. Chanteloup, E. A. Chowdhury, A. Galvanauskas, L. A. Gizzi, J. Hein, D. I. Hillier *et al.*, Petawatt and exawatt class lasers worldwide, High Power Laser Sci. Eng. **7**, e54 (2019).

[23] V. I. Ritus, Quantum effects of the interaction of elementary particles with an intense electromagnetic field, J. Sov. Laser Res. **6**, 497 (1985).

[24] B. S. Xie, Z. L. Li, and S. Tang, Electron-positron pair production in ultrastrong laser fields, Matter Radiat. Extremes **2**, 225 (2017).

[25] A. Di Piazza, C. Müller, K. Z. Hatsagortsyan, and C. H. Keitel, Extremely high-intensity laser interactions with fundamental quantum systems, Rev. Mod. Phys. **84**, 1177 (2012).

[26] G. Sarri, K. Poder, J. M. Cole, W. Schumaker, A. Di Piazza, B. Reville, T. Dzelzainis, D. Doria, L. A. Gizzi, G. Grittani, S. Kar, C. H. Keitel, K. Krushelnick, S. Kuschel, S. P. D. Mangles, Z. Najmudin, N. Shukla, L. O. Silva, D. Symes, A. G. R. Thomas *et al.*, Generation of neutral and high-density electron-positron pair plasmas in the laboratory. Nat. Commun. **6**, 6747 (2015).

[27] J. M. Cole, K. T. Behm, E. Gerstmayr, T. G. Blackburn, J. C. Wood, C. D. Baird, M. J. Duff, C. Harvey, A. Ilderton, A. S. Joglekar, K. Krushelnick, S. Kuschel, M. Marklund, P. McKenna, C. D. Murphy, K. Poder, C. P. Ridgers, G. M. Samarin, G. Sarri, D. R. Symes *et al.*, Experimental Evidence of Radiation Reaction in the Collision of a High-Intensity Laser Pulse with a Laser-Wakefield Accelerated Electron Beam, Phys. Rev. X **8**, 011020 (2018).

[28] K. Poder, M. Tamburini, G. Sarri, A. Di Piazza, S. Kuschel, C. D. Baird, K. Behm, S. Bohlen, J. M. Cole, D. J. Corvan, M. Duff, E. Gerstmayr, C. H. Keitel, K. Krushelnick, S. P. D. Mangles, P. McKenna, C. D. Murphy, Z. Najmudin, C. P. Ridgers, G. M. Samarin *et al.*, Experimental Signatures of the Quantum Nature of Radiation Reaction in the Field of an Ultraintense Laser, Phys. Rev. X **8**, 031004 (2018).

[29] Y.-Y. Chen, P.-L. He, R. Shaisultanov, K. Z. Hatsagortsyan, and C. H. Keitel, Polarized Positron Beams via Intense Two-Color Laser Pulses, Phys. Rev. Lett. **123**, 174801 (2019).

[30] F. Wan, R. Shaisultanov, Y.-F. Li, K. Z. Hatsagortsyan, C. H. Keitel, and J.-X. Li, Ultrarelativistic polarized positron jets via collision of electron and ultraintense laser beams, Phys. Lett. B **800**, 135120 (2020).

[31] Y.-F. Li, Y.-Y. Chen, W.-M. Wang, and H.-S. Hu, Production of Highly Polarized Positron Beams via Helicity Transfer from Polarized Electrons in a Strong Laser Field, Phys. Rev. Lett. **125**, 044802 (2020).

[32] J. A. Clarke, L. I. Malysheva, R. Dollan, J. B. Dainton, J. Sheppard, W. T. Piggott, W. Gai, J. Groberg, A. A. Mikhailichenko, A. F. Hartin *et al.*, The design of the positron source for the International Linear Collider, Conf. Proc. **C0806233**, WEOBG03 (2008).

[33] E. Esarey, C. B. Schroeder, and W. P. Leemans, Physics of laser-driven plasma-based electron accelerators, Rev. Mod. Phys. **81**, 1229 (2009).

[34] A. Pukhov and J. Meyer-ter Vehn, Laser wake field acceleration: the highly non-linear broken-wave regime, Appl. Phys. B: Lasers Opt. **74**, 355 (2002).

[35] W. Lu, C. Huang, M. Zhou, W. B. Mori, and T. Katsouleas, Nonlinear Theory for Relativistic Plasma Wakefields in the Blowout Regime, Phys. Rev. Lett. **96**, 165002 (2006).

[36] S. Corde, E. Adli, J. M. Allen, W. An, C. I. Clarke, C. E. Clayton, J. P. Delahaye, J. Frederico, S. Gessner, S. Z. Green, M. J. Hogan, C. Joshi, N. Lipkowitz, M. Litos, W. Lu, K. A. Marsh, W. B. Mori, M. Schmeltz, N. Vafaei-Najafabadi, D. Walz *et al.*, Multi-gigaelectronvolt acceleration of positrons in a self-loaded plasma wakefield, Nature (London) **524**, 442 (2015).

[37] J. Vieira and J. T. Mendonça, Nonlinear Laser Driven Donut Wakefields for Positron and Electron Acceleration, Phys. Rev. Lett. **112**, 215001 (2014).

[38] N. Jain, T. M. Antonsen, and J. P. Palastro, Positron Acceleration by Plasma Wakefields Driven by a Hollow Electron Beam, Phys. Rev. Lett. **115**, 195001 (2015).

[39] S. Diederichs, T. J. Mehrling, C. Benedetti, C. B. Schroeder, A. Knetsch, E. Esarey, and J. Osterhoff, Positron transport and acceleration in beam-driven plasma wakefield accelerators using plasma columns, Phys. Rev. Accel. Beams **22**, 081301 (2019).

[40] T. Silva, L. D. Amorim, M. C. Downer, M. J. Hogan, V. Yakimenko, R. Zgadzaj, and J. Vieira, Stable Positron Acceleration in Thin, Warm, Hollow Plasma Channels, Phys. Rev. Lett. **127**, 104801 (2021).

[41] S. Gessner, E. Adli, J. M. Allen, W. An, C. I. Clarke, C. E. Clayton, S. Corde, J. P. Delahaye, J. Frederico, S. Z. Green, C. Hast, M. J. Hogan, C. Joshi, C. A. Lindström, N. Lipkowitz, M. Litos, W. Lu, K. A. Marsh, W. B. Mori, B. O'Shea *et al.*, Demonstration of a positron beam-driven hollow channel plasma wakefield accelerator, Nat. Commun. **7**, 11785 (2016).

[42] V. Yakimenko, Y. Cai, C. I. Clarke, S. Z. Green, C. Hast, M. J. Hogan, N. Lipkowitz, N. Phinney, G. R. White, and G. Yocky,

FACET-II accelerator research with beams of extreme intensities, in *Proceedings of the 7th International Particle Accelerator Conference* (JACoW, Geneva, 2016), pp. 1067–1070.

[43] See Supplemental Material at http://link.aps.org/supplemental/10.1103/PhysRevResearch.4.L022028 for details on the employed laser fields, on the applied theoretical model, and on the simulation results for other parameters.

[44] T. D. Arber, K. Bennett, C. S. Brady, A. Lawrence-Douglas, M. G. Ramsay, N. J. Sircombe, P. Gillies, R. G. Evans, H. Schmitz, A. R. Bell, and C. P. Ridgers, Contemporary particle-in-cell approach to laser-plasma modelling, Plasma Phys. Controlled Fusion **57**, 113001 (2015).

[45] V. N. Baier, V. M. Katov, and V. S. Fadin, *Radiation from Relativistic Electrons* (Atomizdat, Moscow, 1973).

[46] V. N. Baier, V. M. Katkov, and V. M. Strakhovenko, *Electromagnetic Processes at High Energies in Oriented Single Crystals* (World Scientific, Singapore, 1998).

[47] A. Ilderton, Note on the conjectured breakdown of qed perturbation theory in strong fields, Phys. Rev. D **99**, 085002 (2019).

[48] A. Di Piazza, M. Tamburini, S. Meuren, and C. H. Keitel, Improved local-constant-field approximation for strong-field QED codes, Phys. Rev. A **99**, 022125 (2019).

[49] Y.-F. Li, R. Shaisultanov, K. Z. Hatsagortsyan, F. Wan, C. H. Keitel, and J.-X. Li, Ultrarelativistic Electron-Beam Polarization in Single-Shot Interaction with an Ultraintense Laser Pulse, Phys. Rev. Lett. **122**, 154801 (2019).

[50] Y.-F. Li, R. Shaisultanov, Y.-Y. Chen, F. Wan, K. Z. Hatsagortsyan, C. H. Keitel, and J.-X. Li, Polarized Ultrashort Brilliant Multi-GeV γ Rays via Single-Shot Laser-Electron Interaction, Phys. Rev. Lett. **124**, 014801 (2020).

[51] J. B. Rosenzweig, N. Barov, M. C. Thompson, and R. B. Yoder, Energy loss of a high charge bunched electron beam in plasma: Simulations, scaling, and accelerating wakefields, Phys. Rev. ST Accel. Beams **7**, 061302 (2004).

[52] L. H. Thomas, The motion of the spinning electron, Nature (London) **117**, 514 (1926).

[53] L. H. Thomas, I. The kinematics of an electron with an axis, London, Edinburgh Dublin Philos. Mag. J. Sci. **3**, 1 (1927).

[54] V. Bargmann, L. Michel, and V. L. Telegdi, Precession of the Polarization of Particles Moving in a Homogeneous Electromagnetic Field, Phys. Rev. Lett. **2**, 435 (1959).

[55] J. Thomas, A. Hützen, A. Lehrach, A. Pukhov, L. L. Ji, Y. T. Wu, X. S. Geng, and M. Büscher, Scaling laws for the depolarization time of relativistic particle beams in strong fields, Phys. Rev. Accel. Beams **23**, 064401 (2020).

[56] M. Büscher, A. Hützen, L. L. Ji, and A. Lehrach, Generation of polarized particle beams at relativistic laser intensities, High Power Laser Sci. Eng. **8**, e36 (2020).

[57] J. Vieira, C.-K. Huang, W. B. Mori, and L. O. Silva, Polarized beam conditioning in plasma based acceleration, Phys. Rev. ST Accel. Beams **14**, 071303 (2011).

[58] G. Alexander, J. Barley, Y. Batygin, S. Berridge, V. Bharadwaj, G. Bower, W. Bugg, F.-J. Decker, R. Dollan, Y. Efremenko, V. Gharibyan, C. Hast, R. Iverson, H. Kolanoski, J. Kovermann, K. Laihem, T. Lohse, K. T. McDonald, A. A. Mikhailichenko, G. A. Moortgat-Pick *et al.*, Observation of Polarized Positrons from an Undulator-Based Source, Phys. Rev. Lett. **100**, 210801 (2008).

[59] J. Fleischer, K. Kołodziej, and F. Jegerlehner, Transverse versus longitudinal polarization effects in $e^+e^- \to W^+W^-$, Phys. Rev. D **49**, 2174 (1994).

[60] J. J. Zha, Z. H. Qin, C. Yuan, and P. X. Wang, High energy positron source driven by laser pulses, Nuc. Instrum. Methods Phys. Res. Sect. A **917**, 43 (2019).

[61] E. Voutier, Physics potential of polarized positrons at the Jefferson laboratory, in *Nuclear Theory*, edited by A. I. Georgievia and N. Minkov (Heron, Sofia, 2014), Vol. 33, p. 142.